

Modeling and simulation of the mixing process of fluids in microchannels promoted by acoustic streaming

Susana O. CATARINO^{1*}, João M. MIRANDA², Senentxu LANCEROS-MENDEZ³, Graça MINAS¹

* Corresponding author: Email: scatarino@dei.uminho.pt

¹ Algoritmi Center, University of Minho, Portugal

² Department of Chemical Engineering, Faculty of Engineering, University of Porto, Portugal

³ Center/Department of Physics, University of Minho, Portugal

Abstract This work describes a study on the acoustic streaming phenomenon, for promoting mixing in microfluidic channels. Acoustic microagitation is a solution to overcome the slow molecular diffusion and accelerate chemical reactions, which is essential to the success of microfluidic devices. A preliminary study has been performed on the piezoelectric effect generated by an electroactive polymer and on the compressible flow Navier-Stokes equations. The simulations were based on finite elements numerical methods. It was concluded that the positioning of the transducer influences the pressure distribution over the fluid domain. It was also seen that the Navier-Stokes equations can be expanded as a sum of equilibrium, first and second order values, that describe the damped propagation of acoustic waves and the global flow, respectively. The time average of the first order results corresponds to a force and can be applied as a source term in the second order equations to determine the mean global flow into the microcuvette.

Keywords: Piezoelectricity, Microfluidics, Acoustic Streaming

1. Introduction

Microfluidic devices have been applied in many diagnostic systems [1], since they guarantee the rapid monitoring of patients with high sensitivity, repeatability and precision [2]. These microfluidic systems allow the immediate detection and quantification of a wide range of biomolecules in biological fluids [3, 4], presenting as main advantages the small size and low power consumption for being used as reliable point-of-care devices. They also allow system integration, small volume of samples and reagents and low cost when mass produced [5, 6, 7].

The small dimensions of those devices feature laminar flow (Reynolds number less than 1). Therefore, vortices do not form and molecular diffusion is the main mixing mechanism. As a consequence, mixing is slow, especially for large molecules. The use of a piezoelectric transducer can be a valuable option to overcome this difficulty, since it

produces the acoustic microagitation phenomenon, promoting the mixing of fluids. Figure 1 shows a basic example of a microfluidic mixing system with a T-mixer that incorporates a piezoelectric transducer for improving the mixing process.

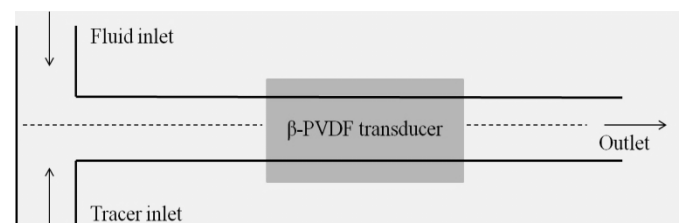


Figure 1. Microfluidic channels system, with two fluid inlets and one outlet. The transducer is a 110 μm film of poly(vinylidene fluoride) in the β phase.

The poly(vinylidene fluoride) – PVDF piezoelectric polymer, in its β phase, can be a suitable material for the generation of acoustic waves. It features good piezoelectric and mechanical properties, as well as low acoustic and mechanical impedance [8], which are

important for the generation and propagation of acoustic waves. The microagitation generated by a piezoelectric transducer is known by acoustic streaming, initially studied by Rayleigh [9, 10], which is based on the absorption of acoustic waves by the fluids, promoting a pressure gradient which generates fluid flow. The harmonic oscillation of the solid boundary near the fluid generates the propagation of the acoustic waves in the fluid as well as a steady mean flow field [10].

The acoustic streaming phenomenon can be divided in two main types: Rayleigh streaming, related to the fluid boundary layers near the solid surfaces and quartz wind, related to the acoustic energy dissipation in the fluid body. The acoustic streaming effects result from the non-linearity of the Navier-Stokes equations, when combined with viscosity [11]. As a result, the required time for mixing the fluids is shorter.

2. Background

Piezoelectricity is a property exhibited by particular materials which, when exposed to mechanical strain in suitable directions, produce an electric polarization proportional to the strain. When the material is subjected to a strain, the molecular structure of the material is deformed, which leads to a different charge distribution on the surface of the material, causing its polarization. So, an electric potential is generated between two electrodes placed on opposite faces of the material (direct effect). The inverse piezoelectric effect occurs when a mechanical strain is produced in response to an external electric field [12, 13].

The inverse piezoelectric effect is a linear phenomenon described by equation (1), where d^T is the piezoelectric coefficient, T the mechanical stress, E the electric field, S the displacement and s_E the elastic coefficient [14].

$$S = s_E T + d^T E \quad (1)$$

The fluid flow can be described by the compressible Navier-Stokes equations, which include the momentum equation (2) and the

continuity equation (3) [15]. ρ is the fluid density, u the velocity field vector, p the pressure, η the dynamic viscosity, κ the dilatational viscosity, F the volume force field and I the identity matrix.

$$\rho \frac{\partial u}{\partial t} + \rho u \cdot \nabla u = \nabla \cdot [-pI + \eta(\nabla u + (\nabla u)^T) - (\frac{2\eta}{3} - \kappa)(\nabla \cdot u)I] + F \quad (2)$$

$$\frac{\partial \rho}{\partial t} + \nabla \cdot (\rho u) = 0 \quad (3)$$

These compressible Navier-Stokes equations are applied since the density varies as a result of pressure changes (due to the compression and decompression of the acoustic waves). The compressible equations are very similar to the incompressible Navier-Stokes equations [15, 16], apart for an extra term in the momentum equation. This term is related to a viscous-stress tensor contribution $(\frac{2\eta}{3} - \kappa)(\nabla \cdot u)I$, which vanishes in incompressible equations since it is assumed that $\nabla \cdot u = 0$ [16, 17].

In order to evaluate the mixing, the mass transport equation must be solved. The mass transport equation is given by (4), where Pe is the Peclet number and c the solute concentration [18].

$$\frac{\partial c}{\partial t} + \vec{v} \cdot \nabla c = \frac{1}{Pe} \Delta c \quad (4)$$

The multiphysics problem constituted by the piezoelectric and the fluid flow equations was computationally solved by finite elements numerical methods. The problem was solved in a simple geometry domain, representing a piezoelectric film of β -PVDF (solid subdomain) under a rectangular microcuvette (fluid subdomain), as shown in figure 2.

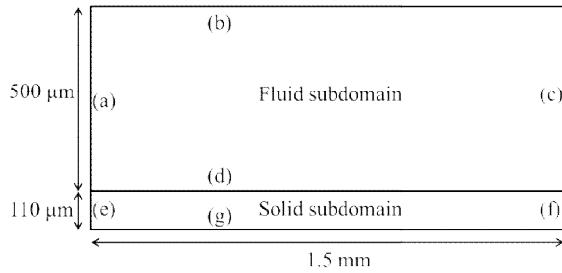


Figure 2. Multiphysics problem domain, representing the solid and fluid subdomains dimensions. The characters (a) to (g) represent the domain boundaries.

The definition of appropriate boundary conditions is essential to the success of the model. Relatively to the solid subdomain, it is necessary to define the mechanical and electrical boundary conditions. Mechanically, the lateral tips (e) and (f) of the β -PVDF film are fixed (displacement is zero), and the upper (d) and lower (g) boundaries are free, which implies that the film vibrates vertically. Electrically, the superior boundary (d) is connected to the ground; the inferior boundary (g) is connected to a sinusoidal voltage of 10 MHz frequency and the lateral boundaries (e) and (f) show electrical continuity. The fluid subdomain refers to a liquid bounded by lateral and superior walls (a), (b) and (c), where the velocity is zero (no slip boundary conditions). The bottom boundary (d) is represented by a mechanical pressure, generated by the piezoelectric effect. The coupling between the solid and liquid domains is based on a continuity approach, i.e. the pressure resulting of the piezoelectric vibration in the solid domain, after each iteration, is applied as a pressure boundary condition in the fluid domain. Moreover, it must be considered the acoustic interface between the transducer and the fluid, since the acoustic reflections at the surface are responsible for a large dissipation of the acoustic pressure. This phenomenon occurs due to the differences between the media acoustic impedances, i.e., the greater the difference, the higher the reflection. The reflected pressure returns to the piezoelectric film as a load applied to the material subdomain.

3 Numerical Approach

This work followed the numerical approach used by Köster [19] and Frampton [20], based on the Navier-Stokes equations.

The main difficulty of this multiphysics phenomenon is the large difference between the time scales. The piezoelectric film vibrates with a frequency of 10 MHz, leading to a time discretization of 1×10^{-7} seconds, while the acoustic streaming relaxation times are about 1×10^{-2} seconds [19]. Therefore, it is necessary to apply an adequate approach to overcome and solve this problem. Accordingly to Köster, two subproblems must be considered separately: acoustics and acoustic streaming.

The numerical study of the acoustics subproblem assumes an expansion of the compressible Navier-Stokes variables (density, pressure and velocity) as a sum of equilibrium (constants in time and space), first order and second order values, taken from the momentum and continuity equations. The first order terms describe the oscillating portion of the variables related to the acoustic field and their time averages are equal to zero. So, these terms represent a linear system that describes the damped propagation of acoustic waves and provide results for the instantaneous flow [19, 20]. The first order system is described by the momentum and continuity equations, respectively:

$$\rho^{(0)} \frac{\partial v^{(1)}}{\partial t} - \nabla \cdot \Sigma^{(1)} = 0 \quad (5)$$

$$\frac{\partial \rho^{(1)}}{\partial t} + \rho^{(0)} \nabla \cdot v^{(1)} = 0 \quad (6)$$

Where $\rho^{(0)}$ represents the equilibrium density, constant in time and space, $\rho^{(1)}$ the first order density, $v^{(1)}$ the first order velocity and the first order value of Σ , which is the Newtonian stress tensor.

Solving this first order system, it is obtained a force, which can be applied as a source term to solve the second order system [19, 20]. After solving the first order system for all the required time steps, it is taken the time average value of the force.

The acoustic streaming subproblem considers the above system solution as known data. This subproblem includes the second order terms and describes the mass and body force sources. The time average values determined above allow analyzing the acoustic streaming effects in a large time scale. Therefore, solving the second order system it is determined the mean global flow [19, 20]. The source term momentum and continuity equations have vector components and are described by the equations:

$$\rho^{(0)} \frac{\partial \bar{v}^{(2)}}{\partial t} - \nabla \cdot \bar{\Sigma}^{(2)} = \langle -\rho^{(1)} \frac{\partial v^{(1)}}{\partial t} - \rho^{(0)} (\nabla v^{(1)}) v^{(1)} \rangle \quad (7)$$

$$\frac{\partial \bar{\rho}^{(2)}}{\partial t} + \rho^{(0)} \nabla \cdot v^{(2)} = \langle -\nabla \cdot (\rho^{(1)} v^{(1)}) \rangle \quad (8)$$

Where $\langle \rangle$ represents the time average, $\rho^{(0)}$ the equilibrium density, $\rho^{(1)}$ the first order density, $\rho^{(2)}$ the second order density, $v^{(1)}$ the first order velocity, $v^{(2)}$ the second order velocity, and $\bar{\Sigma}^{(2)}$ the average of the second order value of Σ .

The 2D model was numerically simulated in COMSOL Multiphysics, since this software allows coupling different physical phenomena, such as piezoelectricity, microfluidics and mass transport. The piezoelectricity and the first order compressible Navier-Stokes equations were solved through the direct SPOLES solver, using a time-dependent approach. It was selected a 1×10^{-10} seconds time step for each simulation.

MATLAB 2010 software was used to post-process the exported COMSOL Multiphysics data and to determine the matrix with the values of the time average source term.

4 Results

As a first approach, the fluid - structure interaction has been studied, which is the coupling of the piezoelectric transducer to the fluid flow, in order to determine the global mean flow and the consequent mixture.

During the study of the piezoelectric effect, generated by the β -PVDF film, it was taken

into account the Rayleigh damping, which value depends on the transducer quality factor and on the resonance frequency. The damping coefficient is given by the Rayleigh equation [21]:

$$c = \alpha m + \beta k \quad (9)$$

Where α is the mass multiplication factor, β the stiffness multiplication factor, c the damping coefficient, m the mass and k the stiffness of the material. As a consequence, the real deformation achieved was lower than the linear equation (1) would predict. Figure 3 displays the total displacement and the first principal stress at the instant $1 \mu\text{s}$, in a two dimensional $110 \mu\text{m}$ β -PVDF film, actuated by a 10 V sinusoidal voltage of 10 MHz frequency. The chosen frequency was 10 MHz since it corresponds to the resonance frequency of the material.

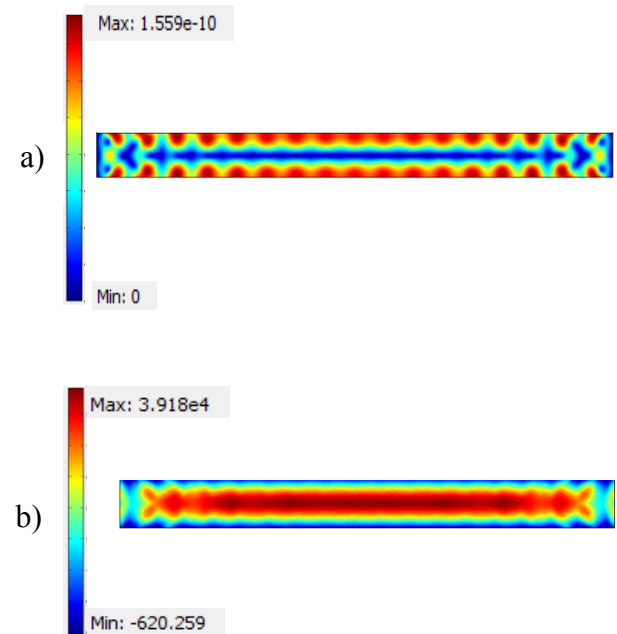


Figure 3. At the instant $1 \mu\text{s}$, in a $110 \mu\text{m}$ thick β -PVDF film, with 1.5 mm length, actuated by a 10 V sinusoidal voltage of 10 MHz frequency. a) Mechanical displacement (m). b) First principal stress (Pa).

Then, the piezoelectric film was coupled to a microcuvette (dimensions $1.5 \text{ mm} \times 500 \mu\text{m}$) filled with water, aiming to determine how the piezoelectric material vibration influences the fluid pressure field. Figure 4 shows the instantaneous distribution of the fluid pressure

in the microcuvette, as a result of the propagation of acoustic waves, as well as the first principal stress in the piezoelectric material.

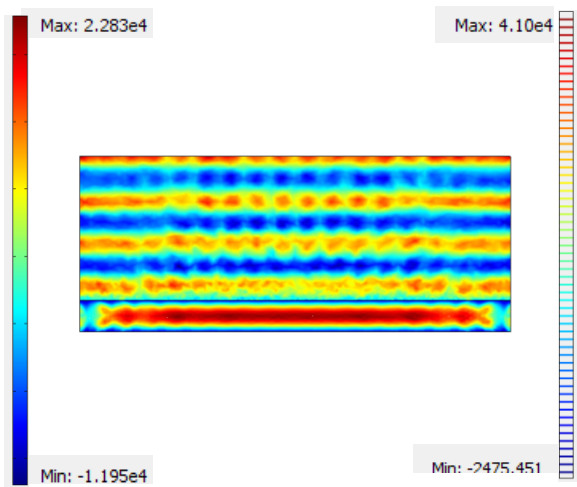


Figure 4. At the instant $1 \mu\text{s}$. *Upper region*: Distribution of the acoustic pressure (Pa), in a fluid microcuvette, over a $500 \mu\text{m} \times 1.5 \text{mm}$ area, when the transducer coupled to its lower wall generates a 10 MHz oscillatory pressure. Each stripe in the figure represents a peak pressure, as a result of the sinusoidal vibration. *Lower region*: Distribution of the first principal stress (Pa) in the $110 \mu\text{m}$ thick β -PVDF film, when an oscillatory electric signal with a frequency of 10 MHz is applied. The vertical colored bars represent the pressure (Pa) color scales in the piezoelectric film (right bar) and in the fluid (left).

The instantaneous pressure in the fluid appears as a succession of peak stripes, alternating maximum and minimum values, as a result of the sinusoidal vibration. These pressure differences allow the movement of the fluids, generating velocity fields in the microcuvette.

Although it is considered a simulation of just $1 \mu\text{s}$, it is enough time to verify changes in the flow field pressure, velocity and forces. Considering the speed of sound in water media (1450 m/s) and its wavelength, as a consequence of the high frequency of the acoustic signal generated by the piezoelectric transducer (10 MHz), it is possible to determine that it takes less than four wave periods (4×10^{-7} seconds) to the acoustic signal reach the upper side of the microcuvette and to reflect part of the acoustic signal.

Replacing the piezoelectric film of 1.5 mm

length by another of 0.5 mm, located under the microcuvette, in a non-centered position, it was possible to study the pressure distribution on the fluid when the pressure boundary condition becomes asymmetric. Figure 5 shows the instantaneous distribution of the fluid pressure in the microcuvette, as a result of the asymmetric propagation of acoustic waves, as well as the first principal stress in the piezoelectric material.

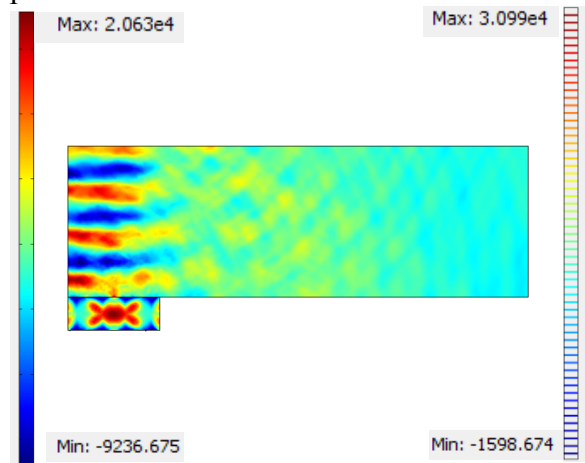


Figure 5. At the instant $1 \mu\text{s}$. *Upper region*: Distribution of the acoustic pressure (Pa), in a fluid microcuvette, over a $500 \mu\text{m} \times 1.5 \text{mm}$ area, when the transducer coupled to its lower wall generates an asymmetric 10 MHz oscillatory pressure. *Lower region*: Distribution of the first principal stress (Pa) in the $110 \mu\text{m}$ thick β -PVDF film, when an oscillatory electric signal with a frequency of 10 MHz is applied.

As it can be clearly seen, in the region above the piezoelectric film, the fluid pressure is displayed in maximum and minimum pressure stripes, similarly to the way it happens when the transducer is located under all the microcuvette. However, out of this region, it is seen that the pressure amplitude decreases with the distance to the acoustic source. Also, there is acoustic reflection on the top and bottom interfaces, creating a zigzag pressure pattern all over the fluid area. This asymmetric transducer geometry seems more appropriate to move and mix the fluids in the microcuvette, once generates a pressure difference over the water, favoring its drive. Figures 6 and 7 show the instantaneous source term in y and x , respectively, at $1 \mu\text{s}$, in the microcuvette with the asymmetric pressure.

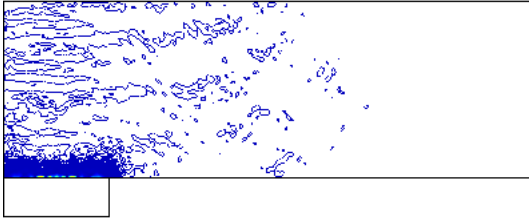


Figure 6. At the instant 1 μ s. Contours distribution of the instantaneous y component of the source term (N/m³) in the microcuvette with the asymmetric pressure.

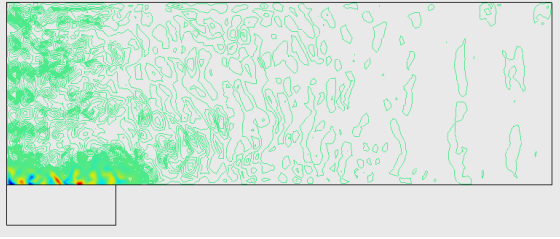


Figure 7. At the instant 1 μ s. Contours distribution of the instantaneous x component of the source term (N/m³) in the microcuvette with the asymmetric pressure.

It can be observed that the source term components distribute over the microcuvette in the same way the fluid pressure is distributed in the domain, which is in agreement to the work developed by Köster [19].

The results are not fully validated yet, since this work comprises only a preliminary study. However, the first results of instantaneous x and y components of source term forces show proximity to the results of Köster [19].

The analytic validation of the acoustic propagation into the microcuvette was performed based on Nabavi work [22]. He developed an equation, based on Navier-Stokes equations, that comprises the physics of sound propagation and boundary conditions, and describes the acoustic propagation of a standing wave into a finite length channel. Nabavi considered a fluid excited by the harmonic motion of a diaphragm, and the analytical solution for the one-dimensional acoustic velocity is given by [22]:

$$u(x, t) = \left(u_0 \sin\left(\frac{\omega'(L-x)}{c}\right) / \sin\left(\frac{\omega'L}{c}\right) \right) \cos \omega t \quad (10)$$

Where x is the distance to the diaphragm, ω

the angular frequency, L the length of the channel, t the sound propagation time, u_0 the vibration speed, c the speed of sound and ω' is given by:

$$\omega' = \omega \left(1 - \frac{3 \delta^2}{2 \omega^2 L^2} \right) \quad (11)$$

Where δ is the dissipation parameter ($\delta < 1$).

Therefore, in order to compare the analytical and numerical models, similar boundary conditions were applied in the COMSOL Multiphysics model. Figure 8 shows the y velocity versus the distance to the acoustic source, considering a 500 μ m height microcuvette and a simulation of 1 μ s.

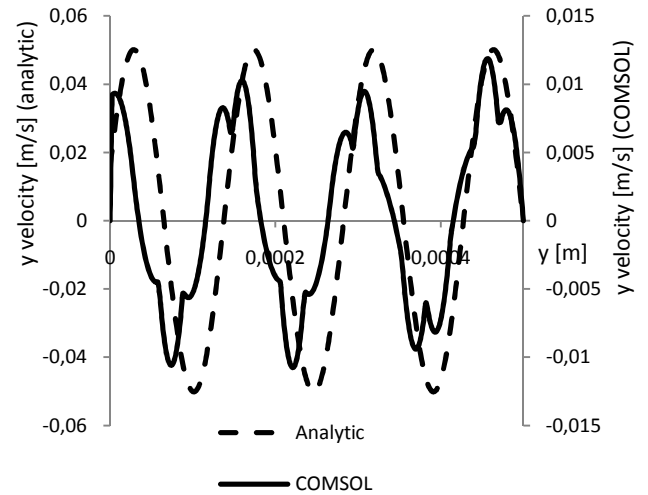


Figure 8. At the instant 1 μ s. Comparison between numerical and analytical results: Distribution of y-velocity (m/s) through the microcuvette height, when an acoustic wave of 10 MHz frequency propagates into water.

The differences between the results can be explained since the analytic method doesn't include the acoustic reflection in the walls, which influences the signals amplitude and is responsible for the signals overtaking, visible in COMSOL Multiphysics results.

Regardless of being just preliminary results, they seem to be in agreement with previous studies on the acoustics and fluidics areas and, therefore, the presented COMSOL Multiphysics model can describe the propagation of sound waves into a fluidic medium.

5 Conclusions and Future Work

The present work evaluated the instantaneous flow in a microcuvette, promoted by an acoustic piezoelectric transducer, after a 1 μ s simulation time.

Although 1 μ s is a short time to evaluate the mixing of fluids, it is enough time to observe changes in the instantaneous flow field parameters (pressure, velocity and body force sources).

It can be concluded that the piezoelectric transducer, when excited with a sinusoidal electric voltage, generates a pressure wave in a microcuvette bordered by walls. This pressure wave propagates across the microcuvette, from the bottom to the top, alternating regions of high and low pressure. The phase and wavelength of the acoustic wave influence the thickness and the number of maximum and minimum pressure stripes. If the piezoelectric transducer is located in a non-centered position relatively to the fluid microcuvette, the pressure shows a different distribution around the fluid, being notorious the acoustic reflection on the walls.

Work is ongoing to determine the average global flow in the microcuvette, through the described second order Navier-Stokes equations, to evaluate the mixing promoted by acoustic streaming in a T mixer (figure 1) and to optimize the geometry of the device.

Acknowledgments

Work supported by FEDER funds through the "Programa Operacional Factores de Competitividade – COMPETE" and by national funds by FCT- Fundação para a Ciência e a Tecnologia project reference PTDC/BIO/70017/2006. S. O. Catarino thanks the FCT for the SFRH/BD/61767/2009 grant.

References

[1] Urban, G., 2009. Micro – and nanobiosensors – state of the art and trends, *Measurement Science and Technology*, 20, 1-18.

- [2] Tudos, A. J., Besselink, G. A. J., Schasfoort, R. B. M., 2001. Trends in miniaturized total analysis systems for point-of-care testing in clinical chemistry, *Lab Chip*, 1(2), 83-95.
- [3] Catarino, S. O., Rocha, J. G., Lanceros-Mendéz, S., Correia, R. G., Cardoso, V. F., Minas, G., 2010. Heating of samples by acoustic microagitation for improving reaction of biological fluids, *Proceedings of ISIE2010 – The International Symposium in Industrial Electronics*, IEEE, Bari, Italy, 446-451.
- [4] Kopp, U. M., Crabtree, H. J., Manz, A., 1997. Developments in technology and applications of microsystems, *Current Opinion in Chemical Biology*, 1, 410-419.
- [5] Figeys, D., Pinto, D., 2000. Lab-on-a-chip: a revolution in biological and medical sciences, *Analytical Chemistry*, May, 330-335.
- [6] Srinivasan, V., Pamula, V., Fair, R., 2004. An integrated digital microfluidic lab-on-a-chip for clinical diagnostics on human physiological fluids, *Lab Chip*, 4, 310-315.
- [7] Chow, A., 2002. Lab-on-a-chip: opportunities for chemical engineering, *AIChE Journal*, 48(8), 1590-1595.
- [8] Cardoso, V. F. et al, 2008. Ultrasonic Transducer based on beta-PVDF for Fluidic Microagitation in a Lab-on-a-Chip device, *Advances in Science and Technology*, 57, 99-104.
- [9] Nyborg, W. L., 1998. Acoustic streaming, In: *Nonlinear acoustics*. San Diego, California: Academic Press, 207–31.
- [10] Rayleigh, L., 1896. *The theory of sound*, MacMillan, London.
- [11] Riley, N., 1997. Acoustic Streaming, *Theoret. Comput. Fluid Dynamics*, 10, 349-356.
- [12] Harris, C., Piersol, A., 2002. *Harris' Shock and Vibration Handbook*, Fifth Edition. McGraw-Hill, NY.
- [13] Gantner, A. et al, 2007. Numerical simulation of piezoelectrically agitated surface acoustic waves on microfluidic biochips, *Comput. Visual Sci.*, 10, 145-161.
- [14] Kutz, M., 2002. *Handbook of Materials Selection*. John Wiley & Sons, NY.
- [15] Kreiss, H., Lorenz, J., 2004. *Initial-Boundary Value Problems and the Navier-Stokes Equations*. Soc. for Ind. Appl. Mathematics. Philadelphia.
- [16] Antil, H., Glowinski, R., 2010. Modeling, simulation and optimization of surface acoustic wave driven microfluidic biochips, *Journal of Computational Mathematics*, 28(2), 149-169.
- [17] Rice, S. A., 1959. On the Dilatational Viscosity of Simple Dense Fluids, *Physics of Fluids*, 2, 579-580.
- [18] Miranda, J. M., Oliveira, H., Teixeira, J. A., Vicente, A. A., Correia, J. H., Minas, G., 2010. Numerical study of micromixing combining alternate flow and obstacles, *International Communications in Heat and Mass Transfer*, 37, 581-586.
- [19] Köster, D., 2006. Numerical simulation of acoustic streaming on SAW-driven biochips, PhD Thesis, University of Augsburg, Germany.

- [20] Frampton, K. D., Martin, S. E., Minor, K., 2003. The scaling of acoustic streaming for application in micro-fluidic devices, *Applied Acoustics*, 64, 681-692.
- [21] Nader, G., Silva, E., Adamowski, J., 2004. Effective damping value of piezoelectric transducer determined by experimental techniques and numerical analysis, *ABCM*

Symposium Series in Mechatronics, 1, 271-279.

- [22] Nabavi, M., Siddiqui K., Dargahi, J., 2008. Measurement of the acoustic velocity field of nonlinear standing waves using the synchronized PIV technique, *Experimental Thermal and Fluid Science*, 33, 123-131.